Prompt Merger Collapse and the Maximum Mass of Neutron Stars

A. Bauswein,[1,2] T. W. Baumgarte,[1,3] and H.-T. Janka[1]

[1]*Max-Planck-Institut für Astrophysik, Karl-Schwarzschild-Strasse 1, D-85748 Garching, Germany*
[2]*Department of Physics, Aristotle University of Thessaloniki, GR-54124 Thessaloniki, Greece*
[3]*Department of Physics and Astronomy, Bowdoin College, Brunswick, Maine 04011, USA*

We perform hydrodynamical simulations of neutron-star mergers for a large sample of temperature-dependent nuclear equations of state and determine the threshold mass above which the merger remnant promptly collapses to form a black hole. We find that, depending on the equation of state, the threshold mass is larger than the maximum mass of a nonrotating star in isolation by between 30 and 70 percent. Our simulations also show that the ratio between the threshold mass and maximum mass is tightly correlated with the compactness of the nonrotating maximum-mass configuration. We speculate on how this relation can be used to derive constraints on neutron-star properties from future observations.

Introduction.—Merging neutron stars (NSs) are among the most promising sources of gravitational radiation for the new generation of gravitational wave (GW) interferometers. Detection rates for Advanced LIGO [1] and Advanced Virgo [2] have been estimated to be between 0.4 and 400 events per year [3]. The merger may result either in a black hole with a hot accretion torus or a massive, hot, differentially rotating NS. Compact binary mergers were also suggested as the central engines of short gamma-ray bursts [4,5]. Material that becomes gravitationally unbound during the coalescence may undergo rapid neutron-capture nucleosynthesis and contribute to the galactic enrichment by heavy, neutron-rich elements [5,6]. The heat release by the radioactive decay of the nucleosynthesis products may also power electromagnetic counterparts [7–9], which are already being searched for [10,11].

The dynamics and observable signatures of a NS merger depend on the binary masses $M_{1,2}$ and the equation of state (EoS) [12–25] (see also Refs. [26–28] for reviews). At nuclear densities, the EoS is not completely known (see, e.g., Ref. [29]) but plays a crucial role in determining the immediate outcome of coalescence. For sufficiently low-mass binaries, the merger results in a stable NS. For more massive binaries, the remnant will ultimately form a black hole. In the *delayed-collapse* scenario, the two stars form a single, differentially rotating merger remnant that is temporarily supported against gravitational collapse by centrifugal and thermal effects [30,31]. Viscous processes, radiation of GWs, and emission of neutrinos redistribute and reduce the remnant's angular momentum and energy, prompting a delayed collapse on a secular time scale. Alternatively, the merger may lead to an immediate, *prompt collapse* on a dynamical time scale. Such a collapse is triggered for more massive binaries, whose total mass $M_{tot} = M_1 + M_2$ cannot be stabilized. For a given EoS, one can thus define a threshold binary mass M_{thres} that separates the two scenarios of prompt and delayed

collapse. The former occurs for $M_{tot} > M_{thres}$, while a dynamically stable remnant is formed for $M_{tot} < M_{thres}$.

It is intuitive to assume that M_{thres} scales with the maximum mass M_{max} of isolated, nonrotating NSs [20]

$$M_{thres} = kM_{max}. \qquad (1)$$

Here, M_{max} is determined by the EoS and can be found by integrating the Tolman-Oppenheimer-Volkoff (TOV) equations (equations of relativistic hydrostatic equilibrium) [32,33]. The coefficient k also depends on the EoS, or equivalently, on NS properties [12–14,20].

In this Letter, we adopt a large set of temperature-dependent, nuclear EoSs in numerical simulations of binary neutron-star mergers to examine the dependence of k on the EoS and to establish a relation between M_{thres} and M_{max}. We focus on equal-mass binaries but also comment on asymmetric systems below. We find that k is tightly correlated with the compactness $C_{max} = (GM_{max})/(c^2 R_{max})$ of the maximum-mass TOV configuration (G is the gravitational constant and c the speed of light). We provide a simple, analytical model to motivate such a correlation and discuss how our results can be used to constrain NS properties, in particular, M_{max}, from future observations. For a given EoS, our findings predict which binary systems undergo prompt or delayed collapse upon merger with corresponding consequences for the postmerger GW signal, the mass ejection during coalescence, and the particular conditions for launching a collimated outflow favorable for a gamma-ray burst (e.g., torus properties and baryon loading of the environment).

Method.—We perform numerical simulations of NS mergers to determine the EoS dependence of M_{thres}, using a 3D relativistic smoothed particle hydrodynamics (SPH) code that employs the conformal flatness approximation of Einstein's field equations and includes a GW backreaction scheme to account for energy and angular momentum losses due to GW emission (see Refs. [15,34,35] for details

TABLE I. Sample of temperature-dependent, nuclear EoSs used in this study. Here $M_{\max}$, $R_{\max}$, $C_{\max}$, and ρ_c are the gravitational mass, areal radius, compactness, and central energy density of the maximum-mass TOV configurations. We list ρ_c in units of the nuclear saturation density $\rho_0 = 2.7 \times 10^{14}$ g/cm³. $R_{1.6}$ is the areal radius of $1.6M_\odot$ NSs. M_{thres} denotes the total binary mass that separates prompt from delayed collapse (see the text). $f_{\text{peak}}^{\text{stab}}$ is the dominant GW frequency in the postmerger phase of the binary with $M_{\text{tot}} = M_{\text{stab}}$, the most massive binary configuration of our sample that does not collapse promptly.

EoS	$M_{\max}$ $(M_\odot)$	$R_{\max}$ (km)	$C_{\max}$	$R_{1.6}$ (km)	M_{thres} $(M_\odot)$	ρ_c/ρ_0	$f_{\text{peak}}^{\text{stab}}$ (kHz)
NL3 [37,38]	2.79	13.43	0.307	14.81	3.85	5.6	2.78
GS1 [39]	2.75	13.27	0.306	14.79	3.85	5.7	2.81
LS375 [40]	2.71	12.34	0.325	13.71	3.65	6.5	3.05
DD2 [38,41]	2.42	11.90	0.300	13.26	3.35	7.2	3.06
Shen [42]	2.22	13.12	0.250	14.46	3.45	6.7	2.85
TM1 [43,44]	2.21	12.57	0.260	14.36	3.45	6.7	2.91
SFHX [45]	2.13	10.76	0.292	11.98	3.05	8.9	3.52
GS2 [46]	2.09	11.78	0.262	13.31	3.25	7.6	3.19
SFHO [45]	2.06	10.32	0.294	11.76	2.95	9.8	3.67
LS220 [40]	2.04	10.62	0.284	12.43	3.05	9.4	3.52
TMA [44,47]	2.02	12.09	0.247	13.73	3.25	7.2	2.96
IUF [38,48]	1.95	11.31	0.255	12.57	3.05	8.1	3.31

of the code). Our study considers 12 microphysical, fully temperature-dependent EoSs with maximum masses in the range of 1.95 to $2.79M_\odot$, which is compatible with the observation of a $1.97M_\odot \pm 0.04M_\odot$ pulsar [36] (see Table I). With the exception of the IUF EoS, these EoSs are also consistent with the detection of a NS with a mass of $2.01M_\odot \pm 0.04M_\odot$ [49]. The radii $R_{\max}$ of the maximum-mass configurations vary between 10.32 and 13.43 km (see also Ref. [23] for the mass-radius relations of most EoSs considered here). The EoSs are chosen without any selection procedure and cover approximately the full range of high-density models regarding their stellar properties. As initial conditions, we set up cold NSs in neutrinoless beta equilibrium on a quasiequilibrium orbit a few revolutions before merging. We assume irrotational stars since tidal locking is unlikely [50,51], and the orbital period is short compared to possible stellar rotation. Unless stated otherwise, we use a resolution of about 340 000 SPH particles.

For each EoS, we determine M_{thres} by performing simulations of binaries with different values of M_{tot}, which is defined as the binary's total gravitational mass at infinitely large binary separation. We focus on equal-mass binaries here and increase M_{tot} in increments of $0.1M_\odot$. We identify M_{stab} with the mass of the most massive binary in our sample with a dynamically stable remnant, i.e., the most massive system that results in a delayed collapse. We similarly identify M_{unstab} with the mass of the least massive binary whose merger triggers prompt collapse. We then estimate $M_{\text{thres}} = (M_{\text{stab}} + M_{\text{unstab}})/2M_\odot \pm 0.05M_\odot$.

Since thermal pressure has an important effect on the collapse behavior (see, e.g., Refs. [31,35,52]), we have

only considered fully temperature-dependent EoSs in this study. Many other simulations instead supplement a barotropic, zero-temperature EoS with a thermal ideal-gas component in order to approximate finite-temperature effects [12–14,19,20,23,26,35]. We have found that in such a "hybrid" treatment the threshold mass M_{thres} depends strongly on the ideal-gas index Γ_{th}. Since Γ_{th} is neither unambiguously defined nor constant [35], fully temperature-dependent EoSs will provide more reliable values for M_{thres} than a hybrid treatment.

In order to calibrate the error introduced by the conformal flatness approximation, we reproduced the fully relativistic simulations of Ref. [20] and found the same collapse behavior in all but one case, for which we obtained a small shift in M_{thres} [53]. We conclude that the effects of the conformal flatness approximation on our results are small. We verified that our resolution with SPH particles is sufficient by reproducing our findings for the DD2 EoS with both 731 000 and 1 202 000 SPH particles. Finally, we reran our simulations for the DD2 EoS starting with different initial binary separations (leading to 2.5, 3.5, and 4.5 orbits before merging) to confirm that this separation does not affect our results.

Results.—The EoS dependence of M_{thres} and k can be expressed by the stellar parameters of nonrotating NSs, which are uniquely determined by the EoS and thus characterize a given EoS. Our survey reveals that k scales very well with the compactness $C_{\max} = (GM_{\max})/(c^2 R_{\max})$ of the maximum-mass configuration of nonrotating NSs (Fig. 1). We find a similarly tight relation when k is expressed as a function of $C_{1.6}^* = (GM_{\max})/(c^2 R_{1.6})$, where $R_{1.6}$ is the radius of a $1.6M_\odot$ NS (see Fig. 1). Since $R_{1.6}$ may be more easily determined than $R_{\max}$, both by future observations [23,29,55,56] and theoretical considerations [57], $C_{1.6}^*$ might be a more useful quantity than $C_{\max}$.

As can be seen in Fig. 1, k is a nearly linear function of $C_{1.6}^*$ in the regime of interest. The maximum residual from the linear fit $k = jC_{1.6}^* + a$ with $j = -3.606$ and
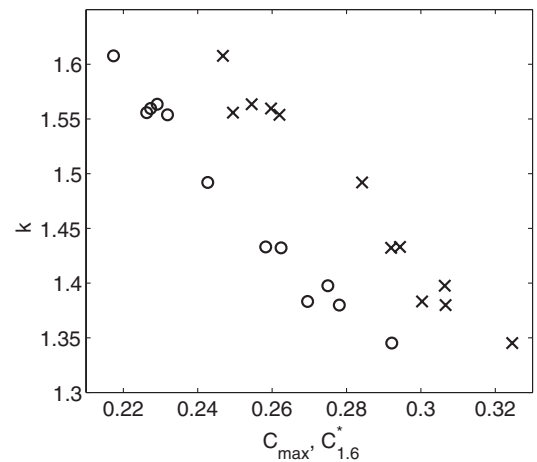

FIG. 1. Coefficient k [Eq. (1)] as a function of $C_{\max} = GM_{\max}/(c^2 R_{\max})$ (crosses) and $C_{1.6}^* = GM_{\max}/(c^2 R_{1.6})$ (circles).

$a = 2.380$ is only 0.025 [58]. By fixing $R_{1.6}$ or R_{max} (see also the discussion of Fig. 3), M_{thres} becomes a quadratic function of M_{max} only. Considering the maximum deviation of k from the fit implies that M_{thres} can be converted to M_{max} with a precision of a few percent for a fixed $R_{1.6}$. An uncertainty of, for instance, 0.5 km in $R_{1.6}$ would add another ~5 percent error. The actual error may be smaller because the deviation of k from the fit includes the intrinsic scatter among different EoSs but also an artificial contribution from the finite sampling of M_{tot} values.

We compared our findings with those of Ref. [20], where six barotropic EoSs with a hybrid treatment of finite-temperature effects were adopted and an approximate relation between k and the radius $R_{1.4}$ of a $1.4 M_\odot$ NS was suggested. Testing this relationship with our extended set of temperature-dependent EoSs results in a distribution with rather wide scattering instead of a tight correlation (see Fig. 2, left panel, and Table I; $R_{1.6}$ is very similar to $R_{1.4}$). However, using the numerical data of Ref. [20] and expressing k as a function of $C_{1.6}^*$ or C_{max} rather than $R_{1.4}$, we found a tight correlation, as for our results. Therefore, we suspect that the approximate scaling with $R_{1.4}$ suggested in Ref. [20] is a selection effect due to the limited number of EoSs used therein [59].

The compactness C_{max} is a measure of the EoS's stiffness at high densities (Fig. 2, right panel; see also Refs. [29,60]), where we characterize the stiffness by the ratio of the mean density $\langle \rho \rangle = 3M_{max}/(4\pi R_{max}^3)$ to the central density ρ_c (i.e., the inverse central condensation). A tight correlation between k and C_{max} thus implies that k depends predominantly on the stiffness of the EoS. This dependence can be motivated qualitatively with the help of a simple Newtonian model. As suggested in Ref. [61], a rough estimate of the fractional increase in the maximum mass $\delta M/M_{max}$ is given by $3T/|W|$, so that $k \approx 1 + 3T/|W|$. Here, T is the rotational kinetic energy and W the potential energy. We compute $T = J^2/(2I)$, where I is the remnant's moment of inertia, from the angular momentum J that the binary carries at the instant of merging. Approximating the merging of an equal-mass binary in circular orbit to occur when the binary separation is twice
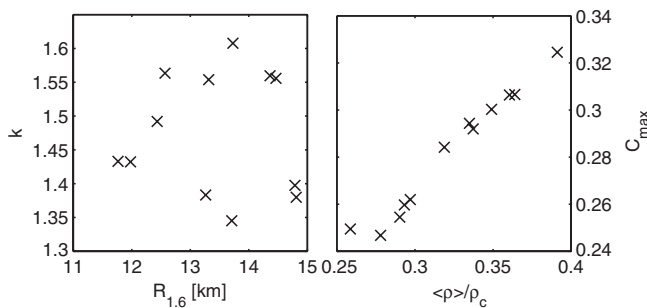
the radius of each individual (spherical) star $R_\star$ and assuming that the progenitors' masses are concentrated at their centers, we find $J^2 \approx GM_{tot}^3 R_\star/8$. Neglecting mass loss as well as deviations from spherical symmetry and assuming that the merger remnant forms a polytrope with polytropic index n, we have $W = -3G/(5-n)M_{tot}^2/R$, where R is the radius of the remnant and $I = 2\kappa_n M_{tot} R^2/5$. Here, the coefficients κ_n depend on n only and are tabulated in Ref. [62]. The EoS's stiffness as well as κ_n increases with decreasing n. Using the polytropic mass-radius relationship for the merging NSs and merger remnant, we also have $R_\star/R = 2^{(n-1)/(3-n)}$. Collecting terms, we now obtain $k \approx 1 + 5(5-n)2^{(n-1)/(3-n)}/(32\kappa_n)$. While this crude approximation overestimates the deviation of k from unity by about a factor of 2, it correctly predicts two important qualitative features of our numerical results: It suggests that k depends predominantly on the EoS's stiffness (since for Newtonian polytropes the stiffness $\langle \rho \rangle / \rho_c$ depends on n only), and it shows that k decreases with increasing stiffness (which can be seen by inserting values for n and κ_n). Loosely speaking, a binary with a stiffer EoS (i.e., a larger $\langle \rho \rangle / \rho_c$) has less angular momentum when merging and its remnant has a larger moment of inertia. These effects combine to decrease $T/|W|$, thereby decreasing k.

For the EoSs in our sample, we also observe a tight correlation between R_{max} and $R_{1.6}$, which implies a close relation between C_{max} and $C_{1.6}^*$.

Observational constraints on the maximum NS mass.— The findings of this study may help to place limits on the maximum mass M_{max} of NSs in the case that future observations, e.g., GW detections, provide an estimate of M_{thres} (cf. Ref. [12]). We assume that delayed and prompt collapse can be distinguished from the presence or absence of GW emission in the 2–4 kHz range produced by the oscillations of the merger remnant, and that the binary mass of the merger can be inferred from the preceding GW inspiral signal, which thus sets a bound on M_{thres}. Depending on the nature of available observations, this information could be used in different ways. In the following, we discuss three speculative possibilities.
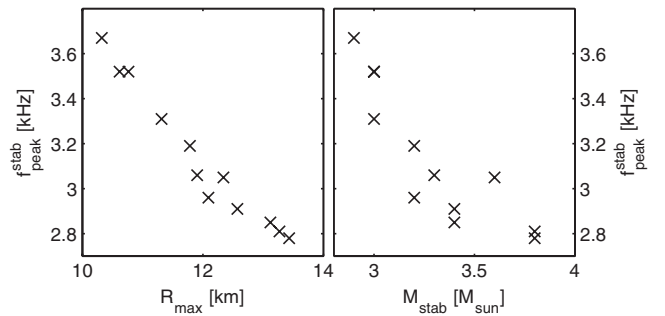

FIG. 2. Left panel: Coefficient k [Eq. (1)] versus radius $R_{1.6}$ of $1.6 M_\odot$ NSs. Right panel: Compactness C_{max} as a function of the EoS's stiffness expressed by the ratio of the average density $\langle \rho \rangle = 3M_{max}/(4\pi R_{max}^3)$ and central energy density ρ_c.

FIG. 3. Dominant GW frequency f_{peak}^{stab} of the postmerger phase for different NS EoSs as function of radius R_{max} (left panel) and M_{stab} (right panel). For each EoS, f_{peak}^{stab} is the frequency f_{peak} for the most massive dynamically stable binary ($M_{tot} = M_{stab}$).

We first assume that a number of detections of NS mergers have been made and that observations of both prompt and delayed collapses bracket M_{thres} to a certain accuracy. If $R_{1.6}$ (or the radius of a NS of any other mass [58]) is independently known to some accuracy, either from future GW measurements (e.g., Refs. [23,55,56]) or astronomical observations [29], then the relation shown in Fig. 1 provides an estimate for the maximum mass of nonrotating NSs in isolation. The accuracy of this estimate depends on the accuracy of M_{thres} and $R_{1.6}$, of course, but since the scatter in the relation between k and $C^*_{1.6}$ is quite small, this scatter will contribute only a few percent of error.

As our second example, we point out that even a single observation of a delayed collapse could provide both an upper and a lower bound on M_{thres}. The lower bound is given immediately by the measured binary mass M_{tot}. An upper bound can be established from the dominant GW frequency f_{peak} of the postmerger oscillations. To show this, we note that f_{peak} increases with increasing binary mass for a given EoS [14,23]. The measured value of f_{peak} therefore provides a lower limit for the peak frequency f^{stab}_{peak} of a binary with the highest total binary mass M_{stab} leading to delayed collapse. In Fig. 3, we show that f^{stab}_{peak} exhibits a tight anticorrelation with R_{max} and a somewhat looser anticorrelation with M_{stab}, which approximates M_{thres}. The lower limit on f^{stab}_{peak} therefore provides an upper limit on both M_{thres} and R_{max}. This means that a measurement of f_{peak} and the binary masses establishes both an upper and a lower limit on M_{thres}, as well as an upper limit on R_{max}. These bounds can then be combined to establish a constraint on M_{max}.

In the third scenario, we again consider just a single detection, but this time we assume that prompt collapse has been established unambiguously. The measured binary mass M_{tot} then forms an upper limit for M_{thres} (as well as a lower limit of $M_{tot}/2$). Without additional information for R_{max} or $R_{1.6}$, the tightest possible constraint on M_{max} is then $M_{max} = M_{thres}/k < M_{tot}/k_{min}$, where k_{min} is the smallest conceivable value of k. For concreteness, consider a 1.5–$1.5 M_\odot$ binary system that leads to prompt collapse. Assuming that our EoS sample covers the full range of high-density models, we have $k_{min} \approx 1.3$. Therefore, a single prompt-collapse detection with $M_{tot} = 3 M_\odot$ leads to the conclusion that $M_{max} \lesssim 3 M_\odot/1.3 \approx 2.3 M_\odot$.

All three of our examples above hinge, of course, on measurements of M_{tot} and/or f_{peak}. Measuring the former requires a relatively large signal-to-noise ratio, since, to leading order, the GW phasing during the inspiral depends on the binary's chirp mass rather than the total mass [63–67]. Since the dominant postmerger GW frequencies are outside of the most sensitive range of the upcoming GW interferometers, detecting these signals will also be possible only for nearby events.

In principle, the precise identification of M_{thres} is problematic because, as M_{tot} approaches M_{thres} from below, the remnant's lifetime becomes increasingly short and the postmerger signal increasingly weak. In practice, however,

the lifetime has a steep sensitivity to the total binary mass. For instance, we find that 8 out of our 12 simulations with $M_{tot} = M_{stab}$ yield remnant lifetimes exceeding 10 ms. This shows that binary systems with masses only slightly below M_{thres} already result in relatively long-lived remnants.

Discussion.—As stated before, we have assumed equal-mass binaries in the above simulations. This assumption is not entirely unjustified, since observations of binary NS systems suggest small mass ratios (see, e.g., Ref. [29] for a review). However, in order to evaluate the effect of unequal masses, we have performed additional simulations with the SFHO, DD2, and NL3 EoSs for binaries with total masses M_{stab} and M_{unstab} (as found from the equal-mass simulations), but now with a mass ratio $q \equiv M_1/M_2 \approx 0.9$. For the given sampling of M_{tot}, we found that symmetric and asymmetric systems of the same total mass show the same collapse behavior. Generalizing our analytical considerations to nonequal masses and expanding the result in deviations from symmetry, $\epsilon \equiv q - 1$ shows that corrections appear at order ϵ^2. This corroborates our numerical finding that moderate deviations of the mass ratio from unity have a small effect on k.

Future work could improve our study in a number of different ways. Even though we expect that the effects of the conformal flatness approximation are small, it would be desirable to perform similar simulations with a fully relativistic treatment. These simulations should also include an even larger sample of temperature-dependent EoSs and should explore the effects of asymmetric binaries.

[1] G. M. Harry and LIGO Scientific Collaboration, Classical Quantum Gravity **27**, 084006 (2010).

[2] F. Acernese, P. Amico, M. Alshourbagy, F. Antonucci, S. Aoudia, S. Avino, D. Babusci, G. Ballardin, F. Barone, L. Barsotti *et al.*, Classical Quantum Gravity **23**, S635 (2006).

[3] J. Abadie *et al.*, Classical Quantum Gravity **27**, 173001 (2010).

[4] S. I. Blinnikov, I. D. Novikov, T. V. Perevodchikova, and A. G. Polnarev, Sov. Astron. Lett. **10**, 177 (1984).

[5] D. Eichler, M. Livio, T. Piran, and D. N. Schramm, Nature (London) **340**, 126 (1989).

[6] J. M. Lattimer, F. Mackie, D. G. Ravenhall, and D. N. Schramm, Astrophys. J. **213**, 225 (1977).

[7] L.-X. Li and B. Paczyński, Astrophys. J. Lett. **507**, L59 (1998).

[8] S. R. Kulkarni, arXiv:astro-ph/0510256.

[9] B. D. Metzger, G. Martínez-Pinedo, S. Darbha, E. Quataert, A. Arcones, D. Kasen, R. Thomas, P. Nugent,

I. V. Panov, and N. T. Zinner, Mon. Not. R. Astron. Soc. **406**, 2650 (2010).

[10] E. Berger, W. Fong, and R. Chornock, Astrophys. J. Lett. **774**, L23 (2013).

[11] N. R. Tanvir, A. J. Levan, A. S. Fruchter, J. Hjorth, K. Wiersema, R. Tunnicliffe, and A. de Ugarte Postigo, Nature (London) **500**, 547 (2013).

[12] M. Shibata, Phys. Rev. Lett. **94**, 201101 (2005).

[13] M. Shibata, K. Taniguchi, and K. Uryū, Phys. Rev. D **71**, 084021 (2005).

[14] M. Shibata and K. Taniguchi, Phys. Rev. D **73**, 064027 (2006).

[15] R. Oechslin, H.-T. Janka, and A. Marek, Astron. Astrophys. **467**, 395 (2007).

[16] M. Anderson, E. W. Hirschmann, L. Lehner, S. L. Liebling, P. M. Motl, D. Neilsen, C. Palenzuela, and J. E. Tohline, Phys. Rev. D **77**, 024006 (2008).

[17] Y. T. Liu, S. L. Shapiro, Z. B. Etienne, and K. Taniguchi, Phys. Rev. D **78**, 024012 (2008).

[18] L. Baiotti, B. Giacomazzo, and L. Rezzolla, Phys. Rev. D **78**, 084033 (2008).

[19] K. Kiuchi, Y. Sekiguchi, M. Shibata, and K. Taniguchi, Phys. Rev. D **80**, 064037 (2009).

[20] K. Hotokezaka, K. Kyutoku, H. Okawa, M. Shibata, and K. Kiuchi, Phys. Rev. D **83**, 124008 (2011).

[21] Y. Sekiguchi, K. Kiuchi, K. Kyutoku, and M. Shibata, Phys. Rev. Lett. **107**, 051102 (2011).

[22] S. Bernuzzi, M. Thierfelder, and B. Brügmann, Phys. Rev. D **85**, 104030 (2012).

[23] A. Bauswein, H.-T. Janka, K. Hebeler, and A. Schwenk, Phys. Rev. D **86**, 063001 (2012).

[24] S. Rosswog, T. Piran, and E. Nakar, Mon. Not. R. Astron. Soc. **430**, 2585 (2013).

[25] A. Bauswein, S. Goriely, and H.-T. Janka, Astrophys. J. **773**, 78 (2013).

[26] M. D. Duez, Classical Quantum Gravity **27**, 114002 (2010).

[27] T. W. Baumgarte and S. L. Shapiro, *Numerical Relativity: Solving Einstein's Equations on the Computer* (Cambridge University Press, Cambridge, England, 2010).

[28] J. A. Faber and F. A. Rasio, Living Rev. Relativity **15**, 8 (2012).

[29] J. M. Lattimer, Annu. Rev. Nucl. Part. Sci. **62**, 485 (2012).

[30] T. W. Baumgarte, S. L. Shapiro, and M. Shibata, Astrophys. J. Lett. **528**, L29 (2000).

[31] J. D. Kaplan, C. D. Ott, E. P. O'Connor, K. Kiuchi, L. Roberts, and M. Duez, arXiv:1306.4034.

[32] R. C. Tolman, Phys. Rev. **55**, 364 (1939).

[33] J. R. Oppenheimer and G. M. Volkoff, Phys. Rev. **55**, 374 (1939).

[34] R. Oechslin, S. Rosswog, and F.-K. Thielemann, Phys. Rev. D **65**, 103005 (2002).

[35] A. Bauswein, H.-T. Janka, and R. Oechslin, Phys. Rev. D **82**, 084043 (2010).

[36] P. B. Demorest, T. Pennucci, S. M. Ransom, M. S. E. Roberts, and J. W. T. Hessels, Nature (London) **467**, 1081 (2010).

[37] G. A. Lalazissis, J. König, and P. Ring, Phys. Rev. C **55**, 540 (1997).

[38] M. Hempel and J. Schaffner-Bielich, Nucl. Phys. **A837**, 210 (2010).

[39] G. Shen, C. J. Horowitz, and S. Teige, Phys. Rev. C **83**, 035802 (2011).

[40] J. M. Lattimer and F. D. Swesty, Nucl. Phys. **A535**, 331 (1991).

[41] S. Typel, G. Röpke, T. Klähn, D. Blaschke, and H. H. Wolter, Phys. Rev. C **81**, 015803 (2010).

[42] H. Shen, H. Toki, K. Oyamatsu, and K. Sumiyoshi, Nucl. Phys. **A637**, 435 (1998).

[43] Y. Sugahara and H. Toki, Nucl. Phys. **A579**, 557 (1994).

[44] M. Hempel, T. Fischer, J. Schaffner-Bielich, and M. Liebendörfer, Astrophys. J. **748**, 70 (2012).

[45] A. W. Steiner, M. Hempel, and T. Fischer, Astrophys. J. **774**, 17 (2013).

[46] G. Shen, C. J. Horowitz, and E. O'Connor, Phys. Rev. C **83**, 065808 (2011).

[47] H. Toki, D. Hirata, Y. Sugahara, K. Sumiyoshi, and I. Tanihata, Nucl. Phys. **A588**, c357 (1995).

[48] F. J. Fattoyev, C. J. Horowitz, J. Piekarewicz, and G. Shen, Phys. Rev. C **82**, 055803 (2010).

[49] J. Antoniadis, P. C. C. Freire, N. Wex, T. M. Tauris, R. S. Lynch, M. H. van Kerkwijk, M. Kramer, C. Bassa, V. S. Dhillon, T. Driebe *et al.*, Science **340**, 448 (2013).

[50] L. Bildsten and C. Cutler, Astrophys. J. **400**, 175 (1992).

[51] C. S. Kochanek, Astrophys. J. **398**, 234 (1992).

[52] V. Paschalidis, Z. B. Etienne, and S. L. Shapiro, Phys. Rev. D **86**, 064032 (2012).

[53] We compared models for the ALF2, SLy4, and APR4 EoSs [54], using a "hybrid" treatment for thermal effects, and found the same behavior as in Ref. [20] for all cases except for APR4, for which we obtained prompt collapse for a 1.42–$1.42 M_\odot$ binary instead of a 1.4–$1.4 M_\odot$ system.

[54] J. S. Read, B. D. Lackey, B. J. Owen, and J. L. Friedman, Phys. Rev. D **79**, 124032 (2009).

[55] J. S. Read, L. Baiotti, J. D. E. Creighton, J. L. Friedman, B. Giacomazzo, K. Kyutoku, C. Markakis, L. Rezzolla, M. Shibata, and K. Taniguchi, Phys. Rev. D **88**, 044042 (2013).

[56] A. Bauswein and H.-T. Janka, Phys. Rev. Lett. **108**, 011101 (2012).

[57] K. Hebeler, J. M. Lattimer, C. J. Pethick, and A. Schwenk, Phys. Rev. Lett. **105**, 161102 (2010).

[58] We found that similar quasilinear relations also hold for C_{max} and for any other $C^* = (GM_{\mathrm{max}})/(c^2 R_{\mathrm{NS}})$, in which NS radii R_{NS} different from those of $1.6 M_\odot$ are used as EoS characterization, e.g., $C^*_{1.4} = (GM_{\mathrm{max}})/(c^2 R_{1.4})$.

[59] The hybrid treatment of thermal effects employed in Ref. [20], with a relatively small value of $\Gamma_{\mathrm{th}} = 1.357$, is likely to underestimate thermal pressure support [35]. This should be taken into account in a direct comparison of the k values.

[60] S. Koranda, N. Stergioulas, and J. L. Friedman, Astrophys. J. **488**, 799 (1997).

[61] N. D. Lyford, T. W. Baumgarte, and S. L. Shapiro, Astrophys. J. **583**, 410 (2003).

[62] D. Lai, F. A. Rasio, and S. L. Shapiro, Astrophys. J. Suppl. Ser. **88**, 205 (1993).

[63] L. S. Finn and D. F. Chernoff, Phys. Rev. D **47**, 2198 (1993).

[64] C. Cutler and É. E. Flanagan, Phys. Rev. D **49**, 2658 (1994).

[65] K. G. Arun, B. R. Iyer, B. S. Sathyaprakash, and P. A. Sundararajan, Phys. Rev. D **71**, 084008 (2005).

[66] M. Hannam, D. A. Brown, S. Fairhurst, C. L. Fryer, and I. W. Harry, Astrophys. J. Lett. **766**, L14 (2013).

[67] J. Aasi, J. Abadie, B. P. Abbott, R. Abbott, T. D. Abbott, M. Abernathy, T. Accadia, F. Acernese *et al.* (The LIGO Scientific Collaboration and The Virgo Collaboration), Phys. Rev. D **88**, 062001 (2013).